Extraction of Prestin-Dependent and Prestin-Independent Components from Complex Motile Responses in Guinea Pig Outer Hair Cells

Nozomu Matsumoto and Federico Kalinec
Section on Cell Structure and Function, Gonda Department of Cell and Molecular Biology, House Ear Institute, Los Angeles, California 90057

ABSTRACT Electromotility of cochlear outer hair cells (OHC) is associated with conformational changes in the integral membrane protein prestin. We have recently reported that electrical stimulation evokes significant prestin-dependent changes in the length, width, and area of the longitudinal section of OHCs, but not in their volume. In contrast, prestin-independent responses elicited at constant membrane potential are associated with changes in cell length, width, and volume without significant changes in their longitudinal section area. In this report we describe a novel analytical technique, based on a simple theoretical model and continuous measurement of changes in cell length and longitudinal section area, to evaluate the contribution of each one of these mechanisms to the motile response of OHCs. We demonstrate that if the relative change in OHC length (L) during the motile response is expressed as $L = A^2 \times V^{-1}$ (with A and V being the relative changes in longitudinal section area and volume, respectively), A^2 will describe the contribution of the prestin-dependent mechanism whereas V^{-1} will describe the contribution of the prestin-independent mechanism. Thus, relative changes in any two of these cellular morphological parameters (L, A, or V) would be necessary and sufficient for characterizing any OHC motile response. This simple approach provides access to information previously unavailable, and may become a novel and important tool for increasing our understanding of the cellular and molecular mechanisms of OHC motility.

INTRODUCTION

Cochlear outer hair cells (OHC) are cylindrical, with a constant diameter of ~9 μm and a length ranging from ~10 μm in the basal, high-frequency turn of the cochlea to ~100 μm in the apical, low-frequency region (1). Three rows of colonnaded OHCs support the organ of Corti's reticular lamina and regulate its distance to the basilar membrane. Whereas passive mechanical properties of OHCs are crucial for the structural integrity of the cochlea, their ability to reversibly change their shape in response to external stimuli is responsible for the exquisite sensitivity of mammalian auditory organ (2–5). This reversible change in shape is known as ''OHC motility'' (6).

OHC motility has been classically divided into fast and slow, corresponding to time courses in the order of microseconds and seconds, respectively (5). Slow motile responses can be induced by a variety of mechanical and chemical stimuli, and they are usually both ATP and Ca^{2+} dependent (5,7). Fast motility, on the other hand, is frequently identified as ''electromotility'' and associated with voltage-dependent conformational changes in the integral membrane protein ''prestin'' (1–3,8–11). Portraying electromotility only as a fast response, however, may be misleading. For instance, slow changes in the ionic environment of the OHC's plasma membrane may induce slow electromotile responses due to fluctuations in membrane potential (12,13). Recently, we suggested that confusion could be avoided by categorizing OHC motility as either prestin-dependent or prestin-independent (12). Moreover, prestin-dependent changes in OHC length were always associated with changes in cell width and longitudinal section area but without detectable variations in cell volume. In contrast, prestin-independent changes in OHC length were associated with changes in cell width and volume without detectable variations in the area of the longitudinal section. These differences not only support the proposed classification, but also confirm previous assumptions about OHC motility and suggest that an experimental approach could be developed for investigating the simultaneous occurrence of both types of OHC motility and for evaluating the individual contribution of each mechanism to the total cell movement (12).

In this study, we extend and complete our previous work on characterizing prestin-dependent and prestin-independent responses, and describe a novel approach for evaluating their contribution to OHC motility either when present alone, or as a combination. With the single assumption that OHCs' shape can be approached by a cylinder, we show theoretically and experimentally that changes in the relative values of OHC volume (V) and longitudinal section area (A) can be estimated from measurements of relative values of cell length (L) in ''pure'' prestin-dependent or prestin-independent responses. Moreover, relative changes in any two of these cellular morphological parameters (L, A, or V) would be necessary and sufficient for characterizing any OHC motile response. These results expand our understanding of OHC motility and provide a new conceptual and experimental

Submitted April 12, 2005, and accepted for publication September 20, 2005.

Address reprint requests to Federico Kalinec, PhD, Section on Cell Structure and Function, Gonda Dept. of Cell and Molecular Biology, House Ear Institute, 2100 West Third St., Los Angeles, CA 90057. Tel.: 213-353-7030; Fax: 213-273-8088; E-mail: fkalinec@hei.org.

0006-3495/05/12/4343/09 $2.00

doi: 10.1529/biophysj.105.064626

framework for analyzing cell mechanical responses combining both motile processes.

MATERIALS AND METHODS

Isolation of guinea pig outer hair cells

Guinea pigs (200–300 g) were euthanized with CO_2 following procedures approved by the Institutional Animal Care and Use Committee. The cochlear spiral was removed from otic bullae and placed in Leibowitz L-15 (Gibco, Gaithersburg, MD) containing 1 mg/ml collagenase (type IV, Sigma, St. Louis, MO), incubated at 31°C for 3 min, and transferred to a recording chamber (PCCS1, Bioscience Tools, San Diego, CA) on an inverted microscope (Axiovert 135TV, Zeiss, Thornwood, NY). OHCs were mechanically dissociated as previously described (14) in the recording chamber filled with L-15, and observed with Nomarski differential interference contrast optics and a 63×/1.2 C-Apochromat objective (Zeiss). Only cells that met the established criteria for healthy OHCs (15) and were not attached to the bottom of the chamber were used in this study.

Special solutions were used instead of L-15 in some experiments, as indicated in the text. The standard external solution contained (in mM): 150 NaCl, 5 KCl, 2 $CaCl_2$, 1 $MgCl_2$, and 10 HEPES. The high K^+ external solution contained (in mM): 5 NaCl, 150 KCl, 2 $CaCl_2$, 1 $MgCl_2$, and 10 HEPES. These solutions were in turn subdivided into other two by adjusting their osmotic pressures to either standard (324 mOsm with ~10 mM glucose) or hypotonic respect to the standard (~310 mOsm with ~0.5 mM glucose) values. The osmolarity of every solution was measured with a μOsmette 5004 freezing-point osmometer (Precision Systems, Natick, MA), and their pH adjusted to 7.4 with Tris(hydroxymethyl) aminomethane (Tris).

Electrophysiology

Whole-cell voltage clamp was achieved under conventional whole-cell patch techniques at room temperature using an EPC-9 patch-clamp amplifier (HEKA, Lambrecht, Germany). Patch electrodes were made from borosilicate capillary glass (G-1.5, Narishige, Tokyo, Japan) using a P-97 micropipette puller (Sutter Instruments, Novato, CA). Intrapipette solution was composed of (in mM): 150 KCl, 1 $MgCl_2$, 0.1 EGTA, 2 ATP-Mg, 0.1 GTP-Na, and 10 HEPES, pH of which adjusted to 7.2 with Tris. Osmolarity of the intrapipette solution was adjusted with glucose to a value slightly higher than that of the control extracellular solution (typically 314 mOsm), increasing the turgor of the cells being recorded and contributing to prevent OHC's attachment to the substrate. The resistance between the patch electrode filled with this solution and the bath solution was 4–6 MΩ.

Capacitance measurement

Measurements of voltage-dependent nonlinear capacitance (NLC) were performed using the ''software lock-in amplifier'' function included in the Pulse software (HEKA, Lambrecht, Germany). OHCs for capacitance measurements were perfused with a blocking solution containing (in mM): 100 NaCl, 5 KCl, 20 CsCl, 20 tetraethylammonium-Cl, 2 $CoCl_2$, 2 $MgCl_2$, 10 glucose, and 10 HEPES, pH of which adjusted to 7.4 with Tris. The intrapipette solution consisted of (in mM): 140 CsCl, 2 $MgCl_2$, 10 EGTA, and 10 HEPES, pH of which adjusted to 7.2 with Tris. The osmolarity of these solutions was adjusted to 310 mOsm with glucose.

Video analysis and data handling

Images of isolated OHCs were captured in QuickTime video format at standard video resolution (720 × 480 pixels) and frequency (30 frames/s) as previously described (12). The obtained video images were then analyzed offline using Dynamic Image Analysis System (DIAS) software (Soll Technologies, Iowa City, IA) running on a Macintosh G4 computer. First, the cell image was rotated as needed, to place it horizontally on the screen. Then, the DIAS software automatically detected the cell edge, found the cell centroid, and measured its geometrical parameters (Fig. 1). Cell length was defined as the maximum horizontal length (the command ''x bounded width'' in DIAS software) of the detected image. Cell width was measured at the cell centroid (command ''central width''). The area of the optical section was measured as the internal area of the detected cell image (command ''area''). The volume of the cell in each analyzed frame was estimated using the model described in Results (Eq. 4; see also Matsumoto and Kalinec (12)). Data was analyzed using Excel (Microsoft, Redmond, WA) and IGOR Pro (Wavemetrics, Lake Oswego, OR) software.

RESULTS

The model

We assume that OHCs are cylinders (Fig. 1). Microscopic images represent optical sections of the cylinders (OHCs), where their lengths, widths, and section areas can be measured directly. The longitudinal section area (a) at the axis of the cylinder (Fig. 1 *A*, *shaded region*), can be calculated from the values of OHC length (l) and width (w) by

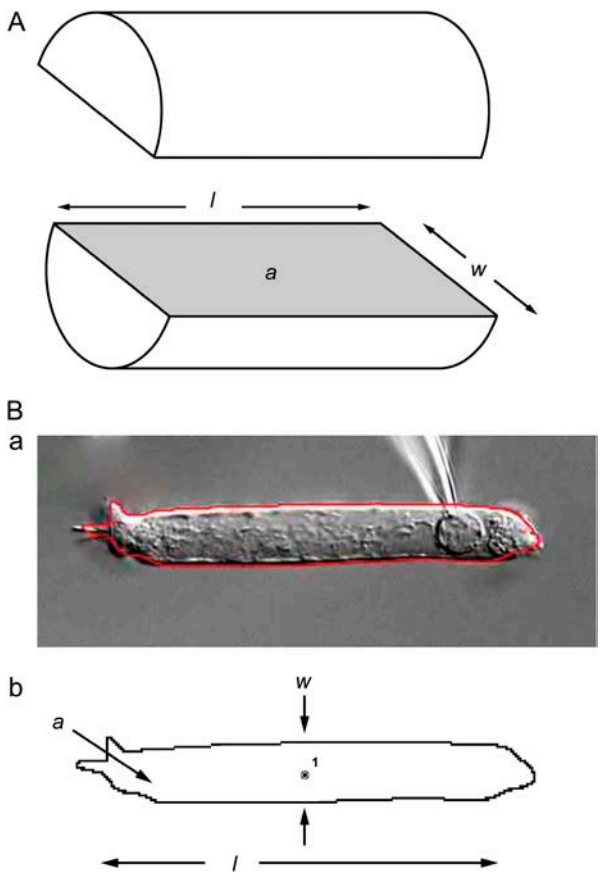

FIGURE 1 Definition of parameters. (*A*) OHCs are modeled as cylinders, and the parameters length (l), width (w), and longitudinal section area (a) are defined as shown in the diagram. (*B*, *a*) Actual picture of an isolated OHC with its automatically defined boundary delineated in red; (*B*, *b*) the automatically defined boundary and the centroid of the cell as measured by DIAS software. The cell width (w) is measured at the cell centroid.

$$a = l \times w \quad (1)$$

The OHC volume (v) can be estimated as

$$v = l \times \pi(w/2)^2 = \pi/4 \times l \times (w)^2 = \pi/4 \times a \times w \quad (2)$$

Equations 1 and 2 may be rewritten for the relative values of length ($L = l_f/l_0$), width ($W = w_f/w_0$), longitudinal section area ($A = a_f/a_0$), and volume ($V = v_f/v_0$)—with the subscripts (0) and (f) identifying the initial and final values, respectively—as

$$A = L \times W \quad (3)$$

and

$$V = L \times W^2 = A \times W \quad (4)$$

From 4, and assuming that prestin-dependent motility is associated only with changes in cell length, width, and longitudinal section area while the cell volume is constant (12), we obtain

$$a_0 \times w_0 = a_f \times w_f (\text{because } v_0 = v_f) \quad (5)$$

thus,

$$w_f = a_0/a_f \times w_0$$

and, using Eq. 4

$$l_f = a_f/w_f = [(a_f/a_0) \times a_0]/[(a_0/a_f) \times w_0] =$$
$$l_f = (a_f/a_0)^2 \times (a_0/w_0) = (a_f/a_0)^2 \times l_0 \quad (6)$$

Then the normalized length change will be:

$$l_f/l_0 = (a_f/a_0)^2$$

or

$$L = A^2 \quad (7)$$

in a ''pure'' prestin-dependent motile response.

Prestin-independent motile responses, on the other hand, would be associated only with changes in OHC length, width, and volume while the longitudinal section area remains constant (12). Thus, $a_0 = a_f$, and from Eqs. 3 and 4

$$v_f/w_f = v_0/w_0 \quad (8)$$

and

$$l_f = a_f/w_f = a_0/w_f = a_0/[(w_f/w_0) \times w_0]$$
$$= (w_0/w_f) \times (a_0/w_0) = (v_0/v_f) \times l_0 \quad (9)$$

Then the normalized length change will be:

$$l_f/l_0 = v_0/v_f = (v_f/v_0)^{-1}$$

or

$$L = V^{-1} \quad (10)$$

in a ''pure'' prestin-independent motile response.

However, OHC motile responses probably are a combination of both prestin-dependent and prestin-independent effects. Therefore, changes in both volume and longitudinal section area should occur simultaneously. Then, from Eqs. 3 and 4

$$a_f/a_0 = (l_f/l_0) \times (w_f/w_0) \quad \text{and} \quad v_f/v_0 = (a_f/a_0) \times (w_f/w_0)$$
$$= (l_f/l_0) \times (w_f/w_0)^2$$

Therefore,

$$(a_f/a_0)^2/(v_f/v_0) = (l_f/l_0)^2 \times (w_f/w_0)^2/(l_f/l_0) \times (w_f/w_0)^2$$
$$= (l_f/l_0)$$

Thus,

$$(l_f/l_0) = (a_f/a_0)^2 \times (v_f/v_0)^{-1}$$

or

$$L = A^2 \times V^{-1} \quad (11)$$

Note that in a ''pure'' prestin-dependent response $V = 1$, and Eq. 7 is recovered. Similarly, in a ''pure'' prestin-independent mechanism $A = 1$, and then Eq. 10 is recovered. Thus, the total cell length change will be equal to the product of the cell length changes induced by the prestin-dependent and prestin-independent mechanisms.

Prestin-independent changes in OHC length are ''volume triggered''

OHCs usually start to decrease in length and increase in width immediately after the rupture of the membrane patch under the voltage-clamp condition (12). This response was associated with changes in cell volume but not in area, indicating a prestin-independent origin. We investigated whether these changes in cell length and volume, which occurred at constant holding potential ($V_H = -70$ mV), obey our model ($L = V^{-1}$, Eq. 10). We found that the inverse value of the estimated changes in cell volume indeed followed very closely the measured values of cell length (Fig. 2 *A*). Moreover, when the pipette solution was turned hypotonic by reducing the amount of glucose, OHCs elongated rather than shortened after membrane rupture. However, the curves describing the changes in L and V^{-1} were again similar (Fig. 2 *B*). Linear correlation analysis of L and V^{-1} data obtained from 10 cells after initial cell length change during whole-cell voltage clamp, confirmed this impression (least squares linear fit: $V^{-1} = 1.06L - 0.09$; $R^2 = 0.91$. Fig. 2 *C*). These results support the hypothesis that prestin-independent OHC motility is associated with volume changes at constant longitudinal section area, and that changes in cell length could be explained as the required adjustment of a cylindrical cell to variations in volume.

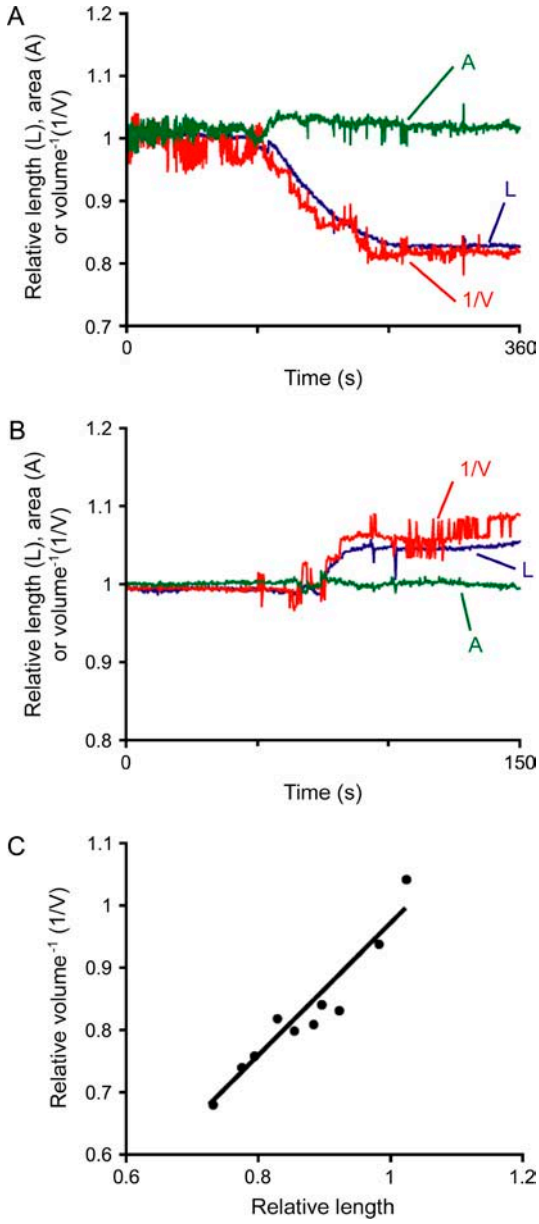

FIGURE 2 Prestin-independent motility. (*A*, *B*) Relative cell length (*L*) and prestin-independent length changes calculated from volume data (1/*V*) in two representative—out of 10—OHCs, either shortened (*A*) or elongated (*B*). *L* and *V* were normalized to the averaged value during the first 10 s of the recording. Note the good fit of *L* and 1/*V*. (*C*) Length changes (in ratio, *x* axis) in function of the inverse value of volume changes (in ratio, 1/*V*, in ratio, *y* axis) from the 10 tested cells. The fit was close to $y = x$. Correlation parameters are: $y = 1.06x - 0.09$, $R^2 = 0.91$.

Prestin-dependent changes in OHC length are ''area triggered''

Electrical stimulation evokes prestin-dependent motile responses in OHCs. Cells change length, width, and area but not volume, at least in an amount detectable with the current resolution of our experimental technique (12). In our model, the relationship between prestin-dependent changes in length and longitudinal section area is expressed by Eq. 7 ($L = A^2$). To test this prediction, we measured morphological parameters in images of electrically stimulated OHCs and investigated whether changes in cell length could be explained as an adjustment to changes in area at a constant cell volume.

First, we confirmed that the motile response was indeed prestin dependent by measuring NLC in OHCs perfused with blocking solution. NLC is widely accepted as the ''electrical signature'' of a prestin-dependent process (3,16–18). Step voltage pulses 100-ms long were applied to OHCs through the patch electrode (from −145 to +95 mV in 15-mV steps), and membrane capacitance was measured at each step (Fig. 3 *A*, *inset*). As expected, cell length and longitudinal section area increased and decreased in response to hyperpolarizing or depolarizing pulses, respectively (Fig. 3 *A*). Membrane capacitance showed typical voltage-dependent nonlinear changes (Fig. 3 *A*, *inset*), indicating prestin activation. Thus, the observed motile responses were associated with prestin activity.

When the values for *L*, *A*, and A^2 were plotted against membrane potential, the curves corresponding to A^2 and *L* were almost identical (Fig. 3 *A*). Moreover, when OHCs received ramp voltage stimulation (from −145 to +50 mV, −65 mV/s), the curves for *L* and A^2, plotted against time, were remarkably similar (Fig. 3 *B*). In a representative OHC, the plot of A^2 against *L* during electrical pulses showed a very strong linear correlation and the values were near the same (least squares linear fit, $A^2 = 1.1L - 0.1$; $R^2 = 0.97$; Fig. 3 *C*). These results support the hypothesis that prestin-dependent OHC motility is associated with area changes at constant cell volume, and that changes in cell length could be explained as the required adjustment of a cylindrical cell to variations in membrane area (12).

Discriminating between prestin-dependent and prestin-independent motile responses

Characterization of prestin-dependent and prestin-independent motility suggests the possibility of identifying and quantifying the individual contribution of each of these mechanisms from a mixed OHC motile response. The total change in OHC length would be the product of the prestin-dependent (A^2) and prestin-independent (V^{-1}) contributions (Eq. 11). Therefore, we measured *L*, *W*, and *A* in a series of experiments to estimate the prestin-dependent and prestin-independent contribution to the total change in cell length.

We first tested the prediction of our model in electrically stimulated OHCs showing ''pure'' prestin-dependent motility as indicated by NLC measurements (Fig. 3 *A*). In this experiment we used 333-ms-long step pulses, rather than the 100-ms-long pulses used before, looking for more frames for video analysis. As predicted, *L* and *A* showed parallel changes during the electrical stimulations (Fig. 4 *A*). The prestin-dependent component (A^2) was near identical to the total change in OHC length (Fig. 4 *B*). In contrast, the

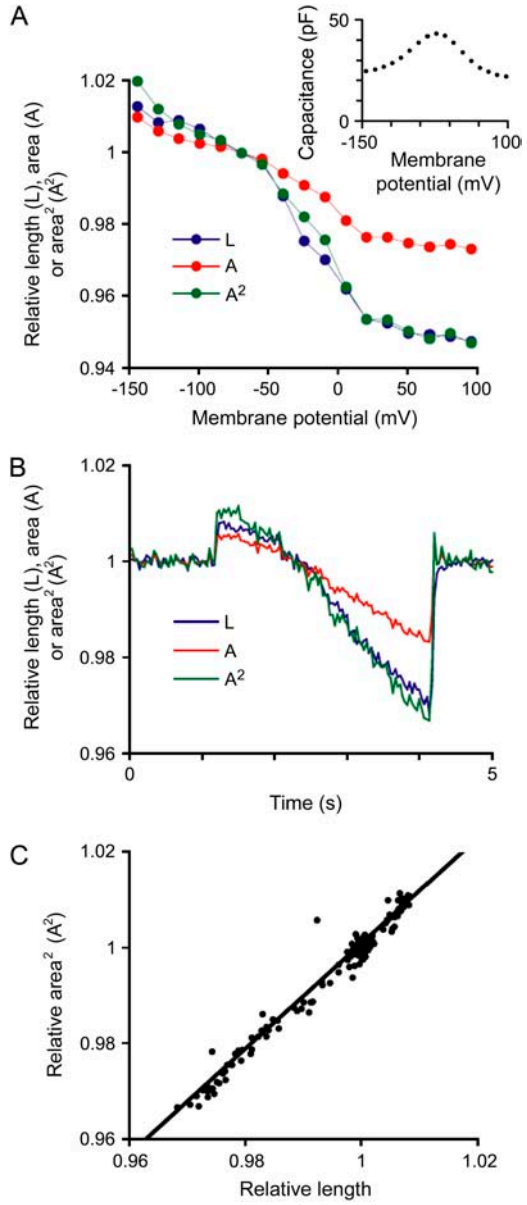

FIGURE 3 Prestin-dependent motility. (*A*) Relative length (*L*, *blue*), longitudinal section area (*A*, *red*), and estimated prestin-dependent length changes calculated from the area values (A^2, *green*) in one representative OHC that underwent square pulse stimulations. The 10 OHCs tested in this experiment showed similar responses. Values were normalized to those during $V_H = -70$ mV and plotted against V_H. Note that actual *L* changes fitted very well with predicted area-triggered length changes (A^2). (*Inset*) Voltage-sensitive nonlinear capacitance measured in this cell. (*B*) Experiments with ramp stimulation. Again, as shown in the response of one representative OHC out of four tested, actual *L* changes fitted very well with predicted area-triggered length changes (A^2). No differences were evident in the response of the four tested OHCs. (*C*) The plot of voltage-induced length changes (*x* axis) to the square value of voltage-induced area changes (A^2, *y* axis) in the same representative cell described in panel *B*. The values were very similar ($y \approx \xi$). Fitting parameters are: $y = 1.1x - 0.09$, $R^2 = 0.97$.

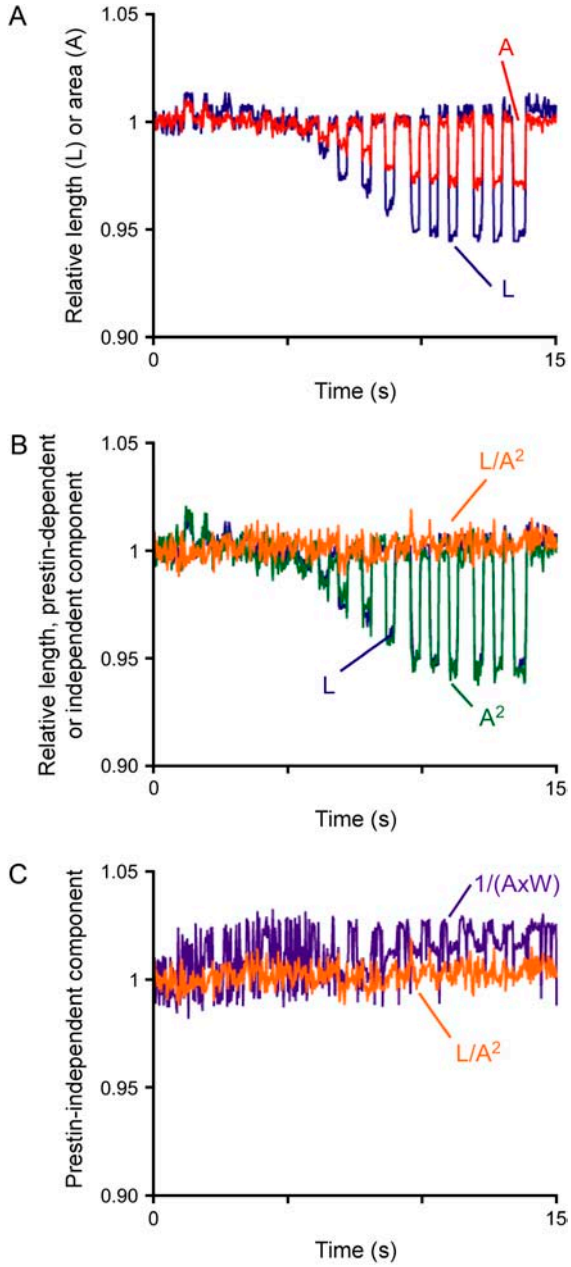

FIGURE 4 Model test of ''pure'' prestin-dependent motility. (*A*) Relative length (*L*, *blue*) and area (*A*, *red*) of a step-pulse-stimulated OHC. Seventeen step pulses, differing in 15 mV, were applied in the range from −145 to +95 mV. Values were normalized to those corresponding to a membrane potential of −70 mV. (*B*) *L* (*blue*), prestin-dependent component (A^2, *green*) and prestin-independent component (L/A^2, *orange*) of the OHC length change shown in panel *A*. Note that *L* is almost perfectly overlapped by A^2 and barely visible, and that no prestin-independent component was apparent. (*C*) Prestin-independent component estimated by two different methods of calculation. Note the overall overlap but differences in noise level.

prestin-independent component V^{-1}, calculated either from *A* and *W* (Eq. 4; $V^{-1} = 1/(A \times W)$) or from *L* and A^2 (Eq. 11; $V^{-1} = L/A^2$), was insignificant as expected (Fig. 4 *C*). These results confirmed that in a ''pure'' prestin-dependent motile

response the total change in OHC length is triggered by area changes.

Next, we induced mixed motile responses by exposing OHCs to high-K^+ solutions of different osmolarity. Whereas K^+ depolarized the plasma membrane triggering prestin-dependent motility, the osmolarity of the extracellular solution did not affect membrane potential but induced prestin-independent motility by changing the cell volume (12). A 324 mOsm glucose-rich solution, instead of L-15, was used during all the steps of OHC isolation and as a control condition. Exposure to a similar solution, but with osmolarity adjusted to 310 mOsm by partial removal of glucose, elicited a slow shortening of the OHCs without detectable changes in their longitudinal section area (Fig. 5 *A*). The high-K^+ (150 mM) solution, in contrast, elicited a decrease in both length and longitudinal section area in OHCs exposed to either 324 mOsm or 310 mOsm solutions. Consistently, the prestin-dependent component (A^2) showed constant changes induced by the depolarizing condition regardless of the underlying osmotic pressure (Fig. 5 *A*). The prestin-independent component calculated as $V^{-1} = L/A^2$ (Eq. 11), on the other hand, was already apparent shortly after the first exposure of the cells to high K^+ solution, and hypotonic solutions elicited only a small additional shortening (Fig. 5 *A*).

To diminish the experimental noise in our data of depolarization-induced mixed motility, we repeated the high K^+ protocol in four OHCs. Only the first application in each cell was analyzed to exclude any remaining slow effect induced by exposure to high K^+. Whereas a decrease in the values of L and A was detected in each OHC in response to exposure to high K^+ solution, the averaged traces for L and A^2 were not similar (Fig. 5 *B*). The decrease in L grew continuously during the perfusion with high K^+, and the recovery after washout was partial. The K^+-induced changes in A^2, in contrast, reached a plateau and the response fully recovered after washout (Fig. 5 *B*). The extracted prestin-independent component (L/A^2) was already visually apparent after ~5 s of depolarization and persisted after washout (Fig. 5 *C*).

Thus, we were able to estimate the individual contribution of both mechanisms to the OHC's mechanical response and, in addition, to analyze independently the effect of different conditions on this contribution.

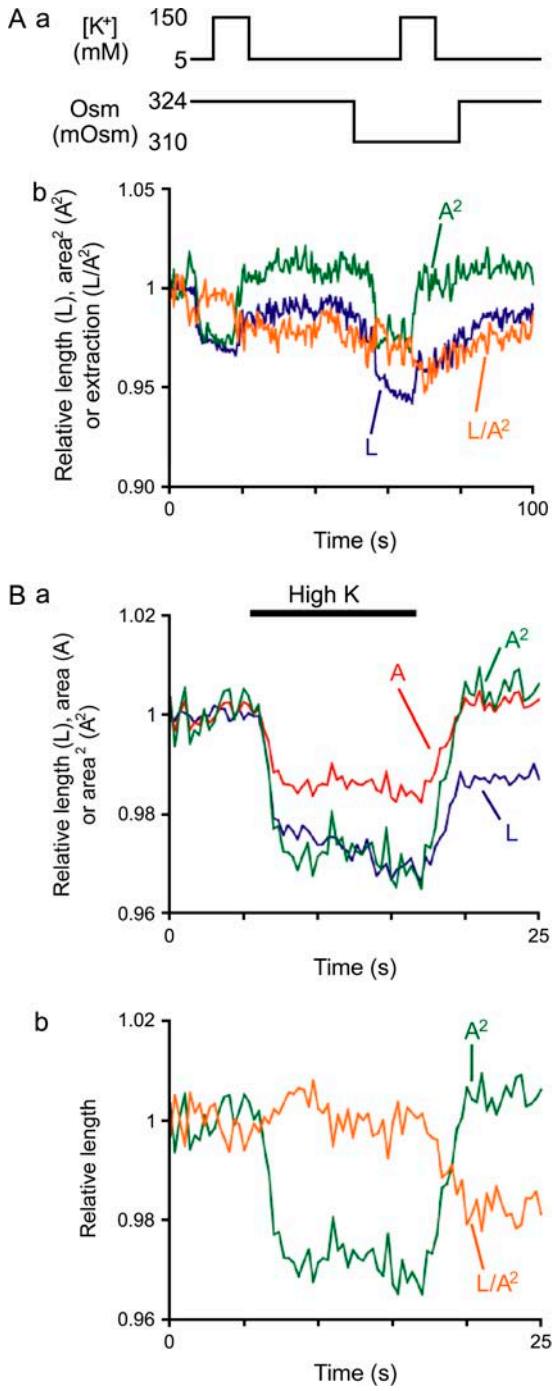

FIGURE 5 Extraction of prestin-dependent and prestin-independent components. (*A*, *a*) Experimental protocol. OHCs were perfused with solutions that differed in K^+ concentration, osmolarity, or both. (*A*, *b*) Relative length (L, *blue*), prestin-dependent length change (A^2, *green*) and prestin-independent length change (L/A^2, *orange*) of one representative OHC. No significant differences in response were observed between the 10 tested OHCs. (*B*) Relative values of L (*blue*), A (*red*), and A^2 (*green*) obtained from four cells during high K^+-induced OHC contraction. L and A were normalized to the averaged values during the first 5 s of the recording. (*C*) Extraction of prestin-dependent and prestin-independent component from the observed L trace in panel *B*.

DISCUSSION

We have described a novel analysis technique based on continuous measurements of changes in length and longitudinal section area to evaluate the individual contribution of prestin-dependent and prestin-independent mechanisms to the motile response of OHCs. A simple theoretical model was developed based on the single assumption that OHCs are cylinders and on experimental results suggesting that prestin-dependent and prestin-independent responses would take place at constant volume and constant longitudinal section

area, respectively (12). Based on this model, we found that if the relative change in OHC length (L) during the motile response is expressed as $L = A^2 \times V^{-1}$ (with A and V being the relative changes in cell longitudinal section area and volume, respectively), A^2 will describe the contribution of the prestin-dependent mechanism whereas V^{-1} will describe the contribution of the prestin-independent mechanism. Experimental results showed that the traces describing changes in length overlap with those corresponding to A^2 and V^{-1} in ''pure'' prestin-dependent and prestin-independent responses, respectively, supporting our hypothesis. Moreover, we were able to identify and quantify the individual contribution of each one of these mechanisms to a mixed OHC motile response. These results suggest that the relative changes in any two of the cellular morphological parameters (L, A, or V) would be necessary and sufficient for characterizing any motile response of isolated OHCs.

The model-based analysis of OHC morphology

Our model is based on the single assumption that the OHC shape is a cylinder. This assumption is not strictly correct, because OHCs have a hemispherical base at the bottom and a cuticular plate at the top that is not perpendicular to the cylinder axis. Although OHCs have been modeled as cylinders in most of the studies published to date (for example, 15,19,20–23), in a few cases more complex models have been used. For instance, the shape of an OHC has been approached by a series of cylindrical segments (24,25), a juxtaposition of a cylinder and a hemisphere (26), a combination of a cylinder, a hemisphere, and 50 small cylinders for stereocilia (27), and even a prolate spheroid (28). These complex models, however, require several additional assumptions. Because modeling the OHC as a cylinder provided values that fitted very well with the actual measurements, we preferred not to add further assumptions and keep the model as simple as possible.

Our model also relies on previous experimental data indicating that electromotile and voltage-independent responses take place at constant volume and constant longitudinal section area, respectively (12). We cannot claim, however, that these parameters are indeed constant but only that the putative changes (if any) are below the sensitivity of our current experimental techniques. Nevertheless, although improved technical approaches might demonstrate that these assumptions are not absolutely true, the relative changes in these parameters should be small enough to be included only as an adjustment factor into the general equations.

A potential pitfall of our experimental approach is that any increase in cell width, such as those associated with the variations in cell volume induced by osmotic challenges, would shift the cell axis from the focal plane, decreasing the values of cell width and longitudinal section area. This problem was already addressed in a previous article (see Appendix in Matsumoto and Kalinec (12)). It can be demonstrated that changes of up to 22% in the original cell diameter will produce undetectable errors in width and longitudinal section area measurements (12). Bigger changes in OHC diameter can be easily identified during image analysis and the focal plane problem mathematically corrected if considered necessary. No corrections were necessary in the experiments reported in this study.

Prestin-independent motility

Prestin-independent changes of up to 30% of initial cell length did not translate into detectable ($\geq$0.7%) changes in longitudinal section area. Because the area of the longitudinal section (a) of a cylinder is strictly proportional to the lateral surface (S) of the cylinder ($S = \pi \times a$), a constant sectional area would indicate that the surface area of the OHC lateral wall is not changing. Therefore, prestin-independent variations in OHC length could be explained as a volume-triggered adjustment of the cell shape at constant membrane area (12). This is consistent with the currently accepted idea that plasma membranes have limited lateral compliance (29,30). The origin of the cell area restriction would be the lipid bilayer component of the membrane, which creates an envelope of nearly fixed area for the cells (30). It is also consistent with data previously reported by other authors —and confirmed in our experiments (results are not shown)—indicating that the two-state Boltzmann fitting of the NLC curve showed a constant linear component (C_{lin}) during cell inflation or deflation (31,32). This hypothesis is further supported by our results indicating that the changes in cell length are inversely proportional to the changes in cell volume, and that the constant of proportionality is practically equal to one (Fig. 2).

Within the limits established by the resolution of our experimental setup, the traces for L and V^{-1} in a ''pure'' prestin-independent response are almost identical. Therefore, direct measurements of changes in cell length could be used as a reliable estimator of the changes in cell volume induced by the prestin-independent motile mechanism. This strategy was already used in estimation of volume changes (33) based on an empirical reverse association of length and volume (34). This may be particularly useful when detection of small changes in volume is required, because of the high resolution of length measurements (see Fig. 2). Of course, this strategy can be applied only if the assumptions of constant area and cylindrical cell shape can be maintained.

Prestin-dependent motility

Electrically evoked prestin-dependent motility is always associated with changes in the longitudinal section area of the cell (12). Changes in the longitudinal section area may represent either actual changes in the surface area of the OHC lateral membrane or variations in submicroscopic membrane bending (12,35,36). This motile response is also characterized by changes in the cell axial stiffness (20,22,

37,38). The covariance of voltage-dependent cell length and stiffness changes strongly suggest that both phenomena are associated with prestin motor function. An important point still unexplained, however, is whether the initial trigger of changes in cell length are the variations in stiffness (stiffness motor, (22)), or in membrane area (area motor, (20)). Although the results of this study do not provide decisive evidence in favor of either one of these two models, they establish an additional condition for the stiffness motor hypothesis. If stiffness is the primary factor in inducing length variations, changes in stiffness must also induce changes in the longitudinal section area of the OHC either by actually changing the membrane area or by alternative mechanisms such as varying the amount of membrane rippling (35,36,39).

Although individual analysis of prestin-dependent quick length changes may not require of the extraction technique described here, it might be necessary for comparing data associated with repetitive stimulations over periods of seconds or longer. In these cases, the analysis of absolute values of electromotile amplitude could be affected by prestin-independent length changes. This problem can be avoided by expressing the changes in electromotile amplitude as a relative value (L) or as a percentage change of total cell length (14,40). Because prestin-dependent changes may be considered isovolumetric, L will provide the total contribution of the prestin-dependent mechanism.

Extraction of prestin-independent contribution from a complex motile response

Slow membrane depolarization evokes both prestin-dependent and prestin-independent motility (12). Because of its time course, however, this type of response has been commonly identified as ''slow motility'' (41,42). Although ''pure'' prestin-dependent or prestin-independent motile responses are probably infrequent at physiological conditions, the analysis of complex motile response has been very difficult to achieve. Our model-based characterization of OHC motility has derived a simple procedure for the identification and quantification of the motility components.

By combining geometrical relationships and actual measurements (Figs. 4 and 5), we demonstrated that the prestin-dependent contribution to the OHC motile response is provided by the term A^2, which can be calculated from direct measurements of the changes in the longitudinal section area of OHCs under microscopic observation. The prestin-independent component (V^{-1}) can be calculated in two different ways, either by removing the area-triggered component from the length changes (Eq. 11; $V^{-1} = L/A^2$), or by using area and diameter measurements (Eq. 4; $V^{-1} = 1/(A \times W)$). In our experimental setup, measurements of L and A provide the more precise values (Fig. 4 C). Therefore, we favored the estimation of the prestin-independent component (V^{-1}) from the relationship $V^{-1} = L/A^2$.

Conclusion

We have described a novel approach for analyzing complex motile responses of isolated OHCs based on simple morphological and experimental considerations. This experimental method provides access to information previously unavailable, and may be very useful for investigating potential synergetic effects of the prestin-dependent and prestin-independent mechanisms. For instance, the proposed functional interaction between the membrane-based force generator mechanism and the underlying actin-spectrin cytoskeleton in OHCs could be directly tested in single experiments. Thus, this experimental approach might become a novel and important tool for increasing our understanding of the cell and molecular mechanisms of OHC motility.

The authors thank Drs. K. Rich, P. Webster, and E. Navarrete for critically reading the manuscript.

This work was made possible by grant No. DC05220 from the National Institute on Deafness and Other Communication Disorders, National Institutes of Health, and the support of House Ear Institute. Its contents are solely the responsibility of the authors and do not necessarily represent the official views of these institutions.

REFERENCES

1. Lim, D. J., and F. Kalinec. 1998. Cell and molecular basis of hearing. *Kidney Int. Suppl.* 65:S104–S113.
2. Santos-Sacchi, J. 2003. New tunes from Corti's organ: the outer hair cell boogie rules. *Curr. Opin. Neurobiol.* 13:459–468.
3. Dallos, P., and B. Fakler. 2002. Prestin, a new type of motor protein. *Nat. Rev. Mol. Cell Biol.* 3:104–111.
4. Nobili, R., F. Mammano, and J. Ashmore. 1998. How well do we understand the cochlea? *Trends Neurosci.* 21:159–167.
5. Dulon, D., and J. Schacht. 1992. Motility of cochlear outer hair cells. *Am. J. Otol.* 13:108–112.
6. Brownell, W. E., C. R. Bader, D. Bertrand, and Y. de Ribaupierre. 1985. Evoked mechanical responses of isolated cochlear outer hair cells. *Science.* 227:194–196.
7. Puschner, B., and J. Schacht. 1997. Calmodulin-dependent protein kinases mediate calcium-induced slow motility of mammalian outer hair cells. *Hear. Res.* 110:251–258.
8. Kalinec, F., M. C. Holley, K. H. Iwasa, D. J. Lim, and B. Kachar. 1992. A membrane-based force generation mechanism in auditory sensory cells. *Proc. Natl. Acad. Sci. USA.* 89:8671–8675.
9. Dallos, P., R. Hallworth, and B. N. Evans. 1993. Theory of electrically driven shape changes of cochlear outer hair cells. *J. Neurophysiol.* 70: 299–323.
10. Hallworth, R., B. N. Evans, and P. Dallos. 1993. The location and mechanism of electromotility in guinea pig outer hair cells. *J. Neurophysiol.* 70:549–558.
11. Zheng, J., W. Shen, D. Z. He, K. B. Long, L. D. Madison, and P. Dallos. 2000. Prestin is the motor protein of cochlear outer hair cells. *Nature.* 405:149–155.
12. Matsumoto, N., and F. Kalinec. 2005. Prestin-dependent and prestin-independent motility of guinea pig outer hair cells. *Hear. Res.* 208: 1–13.
13. Frolenkov, G. I., F. Mammano, and B. Kachar. 2003. Regulation of outer hair cell cytoskeletal stiffness by intracellular Ca2+: underlying mechanism and implications for cochlear mechanics. *Cell Calcium.* 33:185–195.

14. Kalinec, F., M. Zhang, R. Urrutia, and G. Kalinec. 2000. Rho GTPases mediate the regulation of cochlear outer hair cell motility by acetylcholine. *J. Biol. Chem.* 275:28000–28005.

15. Zajic, G., and J. Schacht. 1987. Comparison of isolated outer hair cells from five mammalian species. *Hear. Res.* 26:249–256.

16. Ashmore, J. F., and H. Ohmori. 1990. Control of intracellular calcium by ATP in isolated outer hair cells of the guinea-pig cochlea. *J. Physiol.* 428:109–131.

17. Santos-Sacchi, J. 1991. Reversible inhibition of voltage-dependent outer hair cell motility and capacitance. *J. Neurosci.* 11:3096–3110.

18. Ashmore, J. F. 1990. Forward and reverse transduction in the mammalian cochlea. *Neurosci. Res. Suppl.* 12:S39–S50.

19. Dulon, D., G. Zajic, and J. Schacht. 1990. Increasing intracellular free calcium induces circumferential contractions in isolated cochlear outer hair cells. *J. Neurosci.* 10:1388–1397.

20. Adachi, M., M. Sugawara, and K. H. Iwasa. 2000. Effect of turgor pressure on outer hair cell motility. *J. Acoust. Soc. Am.* 108:2299–2306.

21. Deo, N., and K. Grosh. 2004. Two-state model for outer hair cell stiffness and motility. *Biophys. J.* 86:3519–3528.

22. Dallos, P., and D. Z. He. 2000. Two models of outer hair cell stiffness and motility. *J. Assoc. Res. Otolaryngol.* 1:283–291.

23. Iwasa, K. H. 2000. Effect of membrane motor on the axial stiffness of the cochlear outer hair cell. *J. Acoust. Soc. Am.* 107:2764–2766.

24. Chertoff, M. E., and W. E. Brownell. 1994. Characterization of cochlear outer hair cell turgor. *Am. J. Physiol.* 266:C467–C479.

25. Morimoto, N., R. M. Raphael, A. Nygren, and W. E. Brownell. 2002. Excess plasma membrane and effects of ionic amphipaths on mechanics of outer hair cell lateral wall. *Am. J. Physiol. Cell Physiol.* 282:C1076–C1086.

26. Belyantseva, I. A., G. I. Frolenkov, J. B. Wade, F. Mammano, and B. Kachar. 2000. Water permeability of cochlear outer hair cells: characterization and relationship to electromotility. *J. Neurosci.* 20: 8996–9003.

27. Huang, G., and J. Santos-Sacchi. 1993. Mapping the distribution of the outer hair cell motility voltage sensor by electrical amputation. *Biophys. J.* 65:2228–2236.

28. Santos-Sacchi, J. 1993. Harmonics of outer hair cell motility. *Biophys. J.* 65:2217–2227.

29. Evans, E. A., and D. Needham. 1987. Physical properties of surfactant bilayer membranes: thermal transitions, elasticity, rigidity, cohesion, and colloidal interactions. *J. Phys. Chem.* 91:4219–4228.

30. Mohandas, N., and E. Evans. 1994. Mechanical properties of the red blood cell membrane in relation to molecular structure and genetic defects. *Annu. Rev. Biophys. Biomol. Struct.* 23:787–818.

31. Kakehata, S., and J. Santos-Sacchi. 1995. Membrane tension directly shifts voltage dependence of outer hair cell motility and associated gating charge. *Biophys. J.* 68:2190–2197.

32. Santos-Sacchi, J., W. Shen, J. Zheng, and P. Dallos. 2001. Effects of membrane potential and tension on prestin, the outer hair cell lateral membrane motor protein. *J. Physiol.* 531:661–666.

33. Crist, J. R., M. Fallon, and R. P. Bobbin. 1993. Volume regulation in cochlear outer hair cells. *Hear. Res.* 69:194–198.

34. Dulon, D., J. M. Aran, and J. Schacht. 1988. Potassium-depolarization induces motility in isolated outer hair cells by an osmotic mechanism. *Hear. Res.* 32:123–129.

35. Oghalai, J. S., H. B. Zhao, J. W. Kutz, and W. E. Brownell. 2000. Voltage- and tension-dependent lipid mobility in the outer hair cell plasma membrane. *Science.* 287:658–661.

36. Raphael, R. M., A. S. Popel, and W. E. Brownell. 2000. A membrane bending model of outer hair cell electromotility. *Biophys. J.* 78:2844–2862.

37. He, D. Z., and P. Dallos. 1999. Development of acetylcholine-induced responses in neonatal gerbil outer hair cells. *J. Neurophysiol.* 81:1162–1170.

38. Iwasa, K. H., and M. Adachi. 1997. Force generation in the outer hair cell of the cochlea. *Biophys. J.* 73:546–555.

39. Petrov, A. G. 2002. Flexoelectricity of model and living membranes. *Biochim. Biophys. Acta.* 1561:1–25.

40. Zhang, M., G. M. Kalinec, R. Urrutia, D. D. Billadeau, and F. Kalinec. 2003. ROCK-dependent and ROCK-independent control of cochlear outer hair cell electromotility. *J. Biol. Chem.* 278:35644–35650.

41. Farkas, Z., and I. Sziklai. 2003. Potassium-induced slow motility is partially calcium-dependent in isolated outer hair cells. *Acta Otolaryngol.* 123:160–163.

42. Surin, A. M., U. Reimann-Philipp, and L. D. Fechter. 2000. Simultaneous monitoring of slow cell motility and calcium signals of the guinea pig outer hair cells. *Hear. Res.* 146:121–133.